

Comparison of elementary steps of the cross-bridge cycle in rat papillary muscle fibers expressing α - and β -myosin heavy chain with sinusoidal analysis

Masataka Kawai¹ · Tarek S. Karam¹ · John Jeshurun Michael² · Li Wang^{1,3} · Murali Chandra²

Received: 24 July 2016 / Accepted: 27 September 2016 / Published online: 10 December 2016
© Springer International Publishing Switzerland 2016

Abstract In mammalian ventricles, two myosin heavy chain (MHC) isoforms have been identified. Small animals express α -MHC, whereas large animals express β -MHC, which contribute to a large difference in the heart rate. Sprague–Dawley rats possessing ~99% α -MHC were treated with propylthiouracil to result in 100% β -MHC. Papillary muscles were skinned, dissected into small fibers, and used for experiments. To understand the functional difference between α -MHC and β -MHC, skinned-fibers were activated under the intracellular ionic conditions: 5 mM MgATP, 1 mM Mg²⁺, 8 mM Pi, 200 mM ionic strength, pH 7.00 at 25 °C. Small amplitude sinusoidal length oscillations were applied in the frequency range 0.13–100 Hz (corresponding time domain: 1.6–1200 ms), and effects of Ca²⁺, Pi, and ATP were studied. The results

show that Ca²⁺ sensitivity was slightly less (10–15%) in β -MHC than α -MHC containing fibers. Sinusoidal analysis at pCa 4.66 (full Ca²⁺ activation) demonstrated that, the apparent rate constants were 2–4× faster in α -MHC containing fibers. The ATP study demonstrated that, in β -MHC containing fibers, K_1 (ATP association constant) was greater (1.7×), k_2 and k_{-2} (cross-bridge detachment and its reversal rate constants) were smaller (×0.6). The Pi study demonstrated that, in β -MHC containing fibers, k_4 (rate constant of the force-generation step) and k_{-4} were smaller (0.75× and 0.25×, respectively), resulting in greater K_4 (3×). There were no differences in active tension, rigor stiffness, or K_2 (equilibrium constant of the cross-bridge detachment step). Our study further demonstrated that there were no differences in parameters between fibers obtained from left and right ventricles, but with an exception in K_5 (Pi association constant).

✉ Masataka Kawai
masataka-kawai@uiowa.edu

Tarek S. Karam
tarek-karam@uiowa.edu

John Jeshurun Michael
johnmichael@vetmed.wsu.edu; jjm484@cornell.edu

Li Wang
li-wang-1@suda.edu.cn

Murali Chandra
murali@vetmed.wsu.edu

¹ Departments of Anatomy and Cell Biology, and Internal Medicine, College of Medicine, University of Iowa, Iowa City, IA 52242, USA

² Department of Integrative Physiology and Neuroscience, College of Veterinary Medicine, Washington State University, Pullman, WA 99164-7620, USA

³ School of Nursing, Soochow University, Suzhou 215006, Jiangsu, China

Keywords Myosin heavy chain isoforms · Elementary steps of cross-bridge cycle · Cross-bridge kinetics · Effect of ATP · Effect of Pi · Effect of Ca · pCa-tension · Rigor stiffness

Introduction

Myosin comprises of a family of ATP-dependent motor proteins and they are responsible for actin-based motility. Myosin II is the conventional sarcomeric myosin, which is the major form of skeletal, cardiac, and smooth muscles, and its function is to generate force for contraction. Myosin II is a hexamer consisting of two heavy chains (MHC), and each heavy chain is associated with an essential light chain and a regulatory light chain. In rat cardiac myosin, two MHC isoforms were identified (Pope et al. 1980), and called

α -MHC (fast form with 1938 residues) and β -MHC (slow form with 1935 residues); α - and β -MHC share a sequence identity of 93% with 131 non identical substitutions within the same animal, and the different amino acid residues are clustered in eight segments; of these, four clusters are in subfragment-1 (S1), two clusters in S2, and two more in light meromyosin (LMM) (McNally et al. 1989). The actin-activated ATP hydrolysis rate is 1.2–3 \times faster in fibers containing α -MHC than β -MHC (Michael and Chandra 2015, 2016; Pope et al. 1980). Small animals, such as rodents, carry mostly α -MHC, whereas large animals, such as bovines and humans, carry mostly β -MHC, resulting in a large difference in the heart rate (Lompre et al. 1981; Malmqvist et al. 2004). The heart rate is $\sim 700 \text{ min}^{-1}$ in mice and $\sim 300 \text{ min}^{-1}$ in rats, whereas it is $\sim 70 \text{ min}^{-1}$ in humans. Given these differences, an important question is “*how can we get insights into the problems of human hearts by using rodents as animal models?*”.

To answer this question directly, one method is to compare α -MHC versus β -MHC in the same animal model. We are able to perform this comparison, because it has been known that T_3 (triiodo thyronine) or T_4 (thyroxin) induces the expression of α -MHC, whereas propylthiouracil (PTU) is known to induce the expression of β -MHC (Pagani and Julian 1984; Wang et al. 2013c). Our main question is which elementary steps of the cross-bridge cycle are affected by this myosin isoform shift. While partial results of such comparison have been published on mouse heart fibers (Wang et al. 2013c), a complete comparison has not yet been made. We approached this problem by comparing papillary muscle fibers from normal rats that contain $>99\%$ α -MHC, and those from PTU treated rats that contain 100% β -MHC. Fibers from left ventricle (LV) and right ventricle (RV) were studied independently to determine whether the cross-bridge kinetics are not altered between LV and RV. Our results show that many elementary steps of the cross-bridge cycle are faster in α -MHC containing fibers than those in β -MHC containing fibers. Our results further show that active tension and rigor stiffness were not any different between α -MHC and β -MHC fibers, indicating that the actomyosin interface and series compliance are not affected by the MHC isoform. A difference in cross-bridge kinetics between those expressing α -MHC and β -MHC have been reported previously by Galler et al. (2002).

Methods

Animal protocol

The treatment of animals used in this study followed the guidelines approved by the Institutional Animal Care and

Use Committee of Washington State University. Four month-old male Sprague–Dawley rats were divided in two groups: one consisting of normal rats (designated as WT) that expressed $\sim 99\%$ α -MHC in their ventricles, and the other consisting of propylthiouracil (PTU)-treated rats (designated as PTU) that expressed 100% β -MHC in their ventricles (for biochemical analysis, see Fig. 1). PTU-treatment lasted 4–5 weeks, during which rats were on a solid diet containing 0.15% PTU (Harlan Laboratories, Madison, WI, USA) and water containing 0.2 g PTU/l. Rats used in this study were handled to minimize pain, in compliance with the guideline of the National Academy of Sciences: Guide for the Care and Use of Laboratory animals.

Muscle fiber preparations

PTU treated and WT rats were killed by injection of Na pentobarbital (150 mg/kg), papillary muscles were extracted from both ventricles, and skinned at Washington State University. For skinning procedures and solutions, see Table 1 of Wang et al. (2013b). They were then shipped to University of Iowa in the storage solution (55% glycerol, 45% skinning solution, v/v) on ice for biophysical studies, where they were stored at -20°C . Because there may be a difference in papillary muscles in LV and right ventricle (RV), they were separated and named as LV or RV. Fibers ($\sim 100 \mu\text{m}$ in diameter and $\sim 1 \text{ mm}$ in length) were dissected under the stereo microscope and mounted to the experimental apparatus with two ends fixed with a tiny amount of nail polish to two hooks made of stainless steel wires. One hook was connected to a length driver, and the other to a tension transducer. The fibers were stretched from the slack by 20%, which generally resulted in the sarcomere length of $2.4 \mu\text{m}$.

SDS-PAGE and identification of MHC isoforms

To determine MHC isoform compositions, α - and β -isoforms were separated on a 4% SDS gel at 30 mA for $\sim 20 \text{ h}$, as described previously (Michael et al. 2014). Gels were stained with Bio-Safe Coomassie blue G-250 (Bio-Rad Laboratories, Inc., Hercules, CA), imaged and the percentage of myosin isoforms was determined using ImageJ software (from NIH at: <http://rsbweb.nih.gov/ij/>). The theoretical MW of α -MHC (1938 residues) is 223,511 Da, that of β -MHC (1935 residues) is 223,172 Da, and their difference is 339 Da (McNally et al. 1989).

Solutions and experimental protocol

The experiments included the standard activation study, the rigor study, the MgATP study (referred to as ATP study for simplicity), the P_i study, and the Ca study. The experimental protocol can be seen in Fig. 2. All experiments

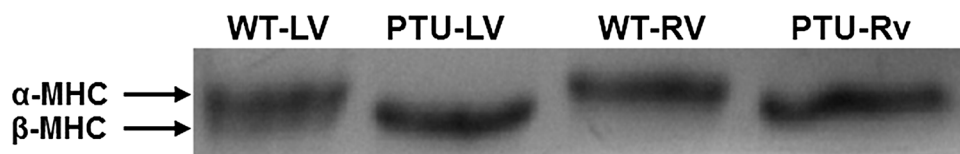


Fig. 1 The results of gel electrophoresis, demonstrating that native (WT) rat heart papillary muscles consist of 99% α -MHC and 1% β -MHC, and that PTU treated rat heart papillary muscles consist of 100% β -MHC as analyzed by NIH Image J software

were performed at 25 °C. The solution compositions used for these studies are as reported (Wang et al. 2014). The standard activating solution included 5 mM MgATP²⁻, 8 mM Pi, 1 mM Mg²⁺, 6 mM CaEGTA²⁻ (*p*Ca 4.66), 15 mM phosphocreatine (PC), 80 units/ml creatine kinase, and pH to 7.00 by 10 mM MOPS. Acetate (Ac) was the major anion, because it preserves muscle fibers better than most other anions (Andrews et al. 1991). Na⁺ concentration was minimized at 55 mM total, for it comes in as Na₂H₂ATP and Na₂CP, and intracellular Na⁺ is at the low mM range (Godt and Maughan 1988). Consequently, the KAc concentration was adjusted to make the ionic strength to 200 mM. Other activating solutions are variations of the above composition by keeping ionic strength at 200 mM. For the *p*Ca study, the total [EGTA] was kept at 6 mM. The calculation of the ionic species including the *p*Ca values and [MgATP] are based on multiple equilibria by using a homemade computer program (ME.exe) with the following apparent association constants at pH 7.00 (mM⁻¹): CaEGTA 1925, MgEGTA 0.041, CaATP 4.99, MgATP 10.1, CaPC 0.014, and MgPC 0.02; other association constants are <0.010 mM⁻¹, and can be ignored.

The ATP, Pi and ADP studies are similar in their general procedures: fibres were tested with the standard activating solution (5 mM MgATP, 8 mM Pi, and 200 mM IS) at the beginning and in the end of experiments (Fig. 2a, d), and rigor was induced following the last activation (Fig. 2e); solutions containing varied [Pi], [Ca²⁺], and [MgATP] were applied (Fig. 2). For the Pi study, its concentrations were 0, 2, 4, 8, 16, and 30 mM, in which 5 mM MgATP

was present (Fig. 2b). For the Ca²⁺ study, its *p*Ca (= -log₁₀[Ca²⁺]) values were 8.0, 7.0, 6.0, 5.9, 5.8, 5.7, 5.6, 5.5, 5.4, 5.3, 5.2, 5.0, and 4.66 in which 8 mM Pi and 5 mM MgATP were present (Fig. 2c). For the ATP study, [MgATP] were 0.05, 0.1, 0.2, 0.5, 1, 2, 5, and 10 mM, in which 8 mM Pi was present (Fig. 2d). In the rigor study, after the last activation with the 10 mM MgATP solution, the rigor solution was applied with two solution changes (Fig. 2e).

Sinusoidal analysis

During tension plateau, sinusoidal analysis was performed to record tension transients as described (Kawai and Brandt 1980; Kawai et al. 1993; Kawai and Zhao 1993; Wang et al. 2014). Frequency (*f*) range used were 0.13–100 Hz, which correspond to 1.6 ms to 1.2 s (= 1/(2π*f*)) in the time domain analysis. The amplitude of the oscillations was kept at 0.125%, which corresponds to ±0.8 nm/cross-bridge with 50% series compliance, and smaller than the cross-bridge’s step size. The complex modulus *Y*(*f*) was calculated as the ratio of tension (stress) change to length (strain) change in the frequency domain.

Elementary steps of the cross-bridge cycle

The data of apparent rate constants 2π*b* and 2π*c* were studied as the functions of [MgATP] and [Pi] at *p*Ca 4.66, and the results were interpreted in terms of Scheme 1. Earlier works have demonstrated that cross-bridges detach

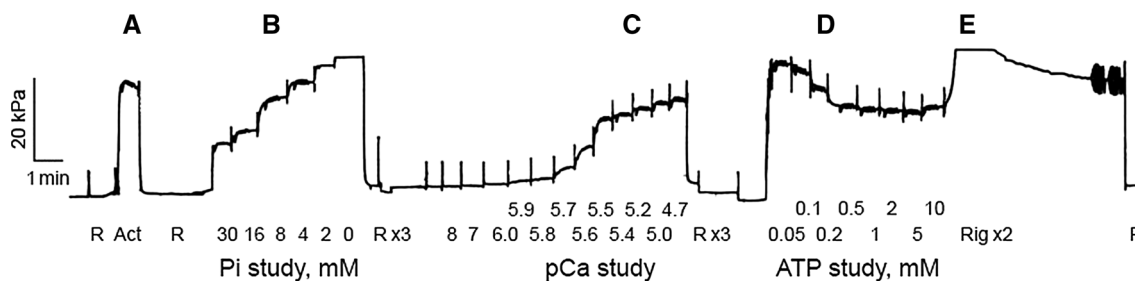
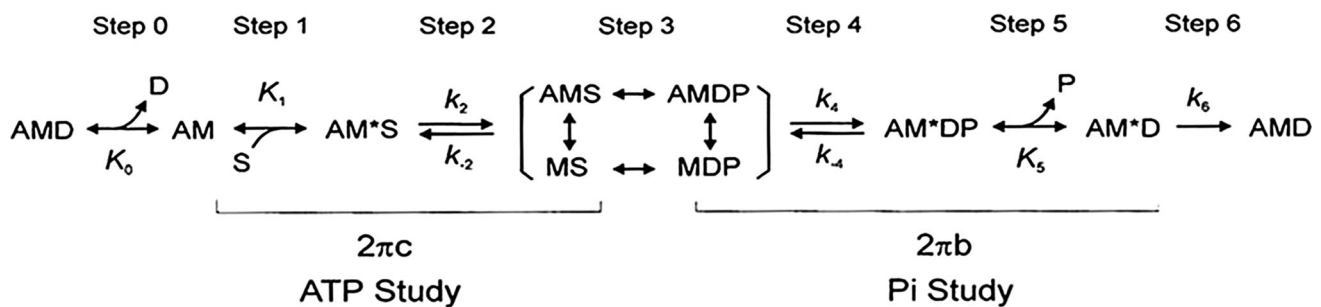


Fig. 2 Representative slow pen trace of isometric tension showing the experimental protocol. A papillary muscle fiber of native (WT) rat heart LV. The standard activation (a) is followed by the Pi study (b), the *p*Ca study (c), and the ATP study (d). Rigor is induced after the

last activation by two solution changes (e). In b and e, tension record was truncated at the top in this pen trace, but the data were recorded correctly in the experimental computer. R relaxing solution, Act standard activating solution, Rig rigor solution



Scheme 1 The cross-bridge model consisting of 6 states, with which the data were interpreted, where *A* actin, *M* myosin, *S* MgATP, *D* MgADP, and *P* Pi phosphate. The *uppercase letters K* indicate

equilibrium constants, whereas *lower case letters k* indicate the rate constants of the elementary step. These are called “kinetic constants”

after binding MgATP; that force generation occurs on step 4 and before Pi is released, based on direct experimental evidence (Caremani et al. 2008; Dantzig et al. 1992; Fortune et al. 1991; Kawai and Halvorson 1991; Tesi et al. 2000). There are opposing views which state that the force is generated with step 5 (Pi release) (Davis and Epstein 2009; Sweeney and Houdusse 2010), but these are based more on theoretical analyses, rather than direct experimental evidence.

Statistical analysis

All the data were presented as mean \pm SE and were analyzed with SPSS 16.0 software. For comparing the difference between WT and PTU mouse types and between LV and RV, a double factor (mouse type and ventricle side) variance analysis was used. $P < 0.05$ was defined to be significant.

Results

SDS-PAGE

To determine MHC isoform compositions, a small piece from the ventricles were solubilized in sample diluting buffer, and gel electrophoresis was performed as described (Michael and Chandra 2016). Figure 1 shows the result. For WT LV, the α -MHC content was $99.03 \pm 0.25\%$ (β -MHC $0.97 \pm 0.25\%$); for WT RV, the α -MHC was $99.58 \pm 0.42\%$ (β -MHC $0.42 \pm 0.42\%$); for PTU LV α -MHC was $100.00 \pm 0.00\%$; and for PTU RV α -MHC was $100.00 \pm 0.00\%$ (\pm SEM, $n = 3$ hearts). These results demonstrate that the ventricles of WT consist of $>99\%$ α -MHC, and the ventricles of PTU-treated rats consist of 100% β -MHC. These values are consistent with those of others (Wang et al. 2013c) in which they found 100% α -MHC in WT and 100% β -MHC in PTU in both mice and rats. The effects of PTU-treatment on the phosphorylation

status of myofilament proteins have been described (Ford and Chandra 2012; Michael et al. 2014).

Active tension

To determine if the ability to generate force is the same between papillary muscle fibers from left and right ventricles, and those containing α -MHC and β -MHC isoforms, the fibers were activated by two solutions: one containing 8 mM Pi, and the other no added Pi. 8 mM Pi is close to the intracellular concentration of working cardiomyocytes (Opie et al. 1971; Roth et al. 1989); the 0 mM Pi solution was also used, because many past experiments have employed this condition [e.g., Miller et al. (2001); Song et al. (2011); Wolska et al. (1999)]. The results are plotted in Fig. 3. This figure demonstrates that the amount of isometric tension generated is not significantly different for left and right ventricles, and for those containing α -MHC and β -MHC isoforms at both 8 mM Pi and 0 mM Pi conditions. Tension in 0 mM Pi is about $2\times$ larger than that in 8 mM Pi solution as expected.

Rigor stiffness

To examine if the mechanical linkage of actin–myosin interface and series compliance are altered in four kinds of preparations, rigor was induced from Ca^{2+} activated preparations by washing out Ca^{2+} . This rigor was called “high rigor state” in our earlier publication (Kawai and Brandt 1976), and it gives the stable and largest rigor stiffness. Other methods of inducing rigor give less and variable stiffness and tension (Kawai and Brandt 1976), which we have avoided. The rigor elastic modulus (stiffness) was measured at 100 Hz and compared in Fig. 4. This figure shows that there is no difference in rigor stiffness among four preparations, indicating that the actin–myosin linkage (and series elastic elements) is the same for left and right ventricles, and for α -MHC and β -MHC.

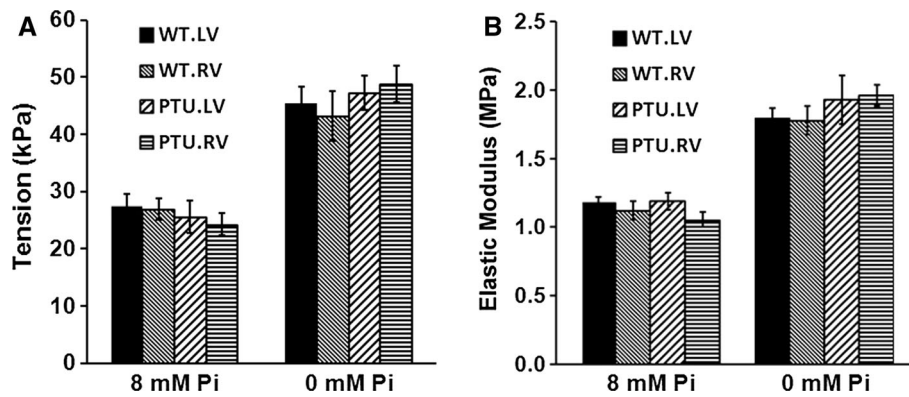


Fig. 3 Active tension (in **a**, kPa) and elastic modulus (stiffness) (in **b**, MPa) are compared among four kinds of preparations with the standard activating solution (8 mM Pi) versus that did not add Pi (0 mM Pi). Resting tension and resting elastic modulus were respectively subtracted from the data. Elastic modulus corresponds

to $Y_{\infty} = H - B + C$. H , B and C are defined in Eq. 1. Error bars indicate SEM; the number of experiments (N) was: WT.LV (23), WT.RV (17), PTU.LV (17), and PTU.RV (22) for tension; WT.LV (23), WT.RV (14), PTU.LV (17), and PTU.RV (21) for elastic modulus. There is no significant difference within each condition

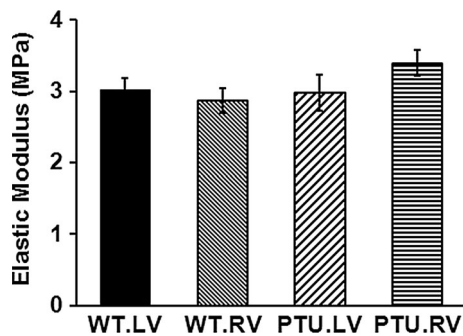


Fig. 4 Elastic modulus (stiffness) of the rigor state, measured at 100 Hz, is compared for the four different preparations. Plotting convention is the same as in Fig. 3. Error bars indicate SEM; the number of experiments (N) was: WT.LV (18), WT.RV (17), PTU.LV (17), and PTU.RV (20). There is no significant difference in rigor elastic modulus among four kinds of preparations

because of a help from actively cycling cross-bridges. From Fig. 5b, it can be seen that the viscous modulus is negative in the low frequency range, indicating that oscillatory work is produced at these frequencies.

The apparent rate constants $2\pi b$ and $2\pi c$ were deduced from fitting $Y(f)$ to Eq. 1, and the results are plotted in Fig. 6. This figure demonstrates that $2\pi b$ of α -MHC containing fibers are $\sim 4\times$ faster than that of β -MHC containing fibers, and that $2\pi c$ of α -MHC containing fibers are $\sim 2\times$ faster than that of β -MHC containing fibers. It also demonstrates that, in α -MHC containing fibers, both rate constants are $\sim 20\%$ faster in RV than in LV. PTU treatment eliminated this natural difference between LV and RV preparations (Fig. 6).

Complex modulus $Y(f)$ during standard activation

Figure 5a plots elastic modulus and Fig. 5b plots viscous modulus against frequency. Figure 5c is the Nyquist plot of $Y(f)$. Papillary fibers taken from LV are compared for normal rats with α -MHC (WT) and PTU-treated rats with β -MHC. It is apparent from these plots that the frequency that gives minimum elastic modulus is shifted horizontally by $\sim 3\times$, and the frequency that gives maximum viscous modulus is shifted horizontally by $\sim 2\times$, indicating that the cross-bridge kinetics are two to three times faster in α -MHC fibers than β -MHC fibers. From plots of Fig. 5, it is also apparent that both elastic and viscous modulus values are smaller in activated fibers than in relaxed fibers in the low frequency range. This is a characteristic property of cardiac muscle preparations, and it indicates that less stiffness is experienced during activation than relaxation,

ATP study

To examine the elementary steps surrounding ATP binding to the myosin head and how the subsequent cross-bridge dissociation are affected by MHC isoform, $[MgATP]$ was changed in the range 0.05 mM and 10 mM in the presence of 8 mM Pi at saturating Ca^{2+} (pCa 4.66) (Fig. 2d), and the complex modulus data $Y(f)$ were obtained at each $[MgATP]$. The apparent rate constant $2\pi c$ was extracted from $Y(f)$ by fitting it to Eq. 1 and plotted in Fig. 7a for four kinds of preparations. $2\pi c$ increased at low mM range of $[MgATP]$, and then saturated at 5–10 mM. There were no significant differences between LV and RV, but $2\pi c$ was $1.7\times$ greater in fibers with α -MHC compared to those with β -MHC. These results were fitted to Eq. 2, which is based on steps 1 and 2 of Scheme 1. This fitting finds the association constant (K_1) of ATP to cross-bridges, the rate constant of cross-bridge detachment step 2 (k_2), and the rate constant of its reversal step (k_{-2}). Their averaged

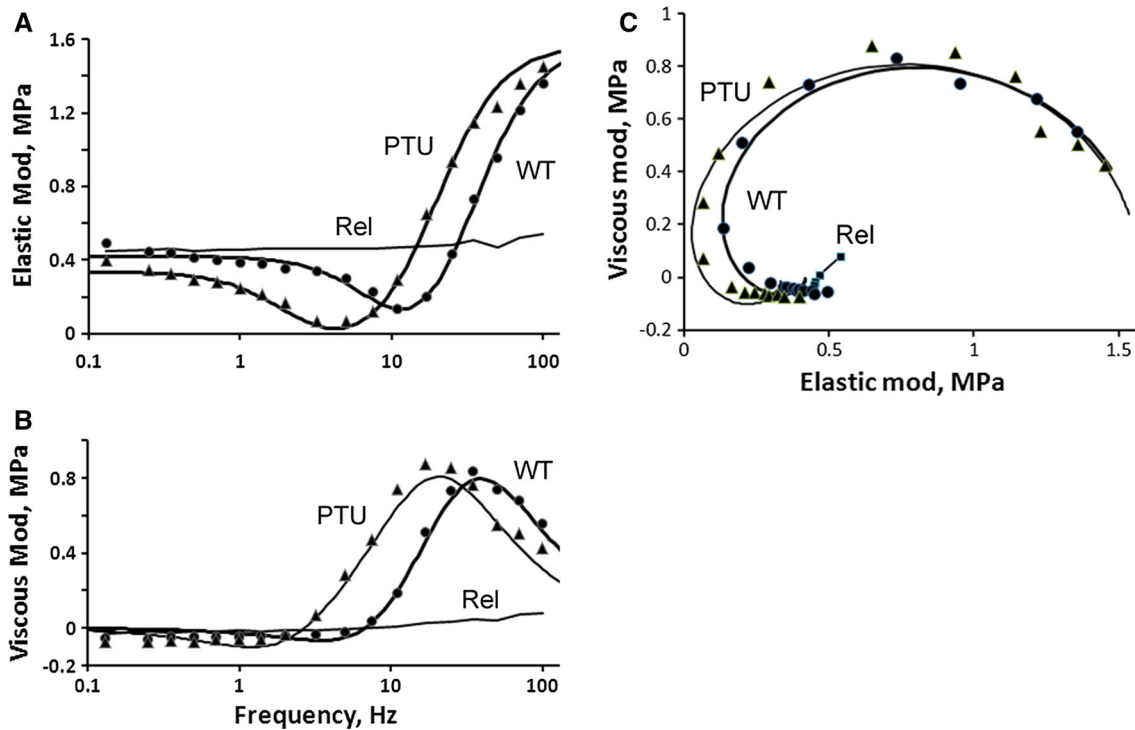


Fig. 5 Plots of complex modulus $Y(f)$ of LV comparing fibers from WT and PTU-treated rats during standard activation. Rel indicates the data from relaxed fibers, which were just about the same for WT and PTU fibers. The data from RV are not shown, for they are not much different from the LV data. **a** Plot of elastic modulus [=Real $Y(f)$] versus frequency, **b** plot of viscous modulus [=Imag $Y(f)$] versus frequency, and **c** plot of viscous modulus versus elastic modulus (Nyquist plot). In **c**, the frequency increases in the clockwise direction for WT and PTU, and Rel (filled square measured during relaxation) includes only

decade frequencies in which 100 Hz point is furthest from the origin. Smooth curves represent best fit of the data to Eq. 1 (Kawai and Brandt 1980; Wannenburg et al. 2000): $Y(f) = H - \frac{Bfi}{b + fi} + \frac{Cfi}{c + fi}$ where $i = \sqrt{-1}$; b and c ($b < c$) are the characteristic frequencies of processes B and C , respectively; B and C are their respective magnitudes (amplitudes), and $2\pi b$ and $2\pi c$ are their respective apparent rate constants. $2\pi b$ and $2\pi c$ respectively correspond to the rate constants of phases 3 and 2 of step analysis (Heinl et al. 1974; Huxley 1974).

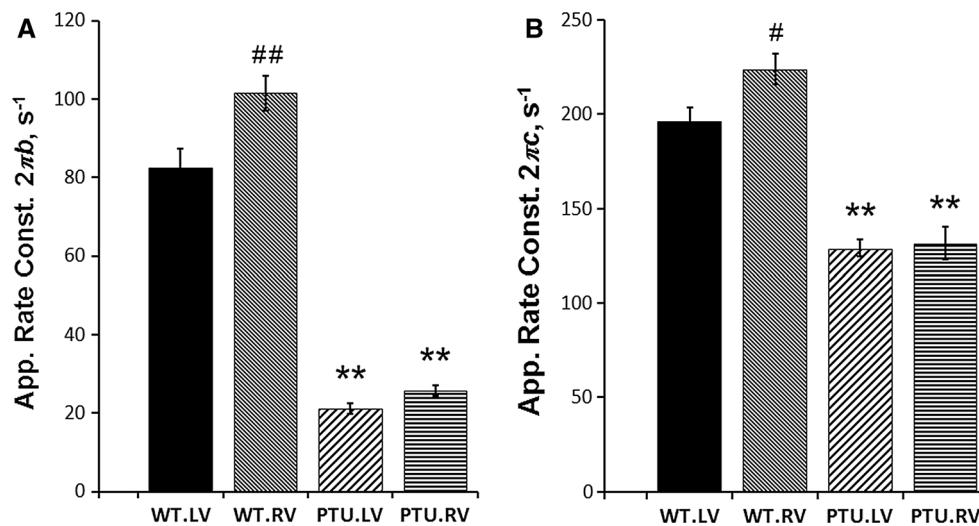


Fig. 6 Apparent rate constants $2\pi b$ (in **a**) and $2\pi c$ (in **b**) during the standard activation are plotted for 4 kinds of fibers. The number of experiments (N) was: WT.LV (30), WT.RV (32), PTU.LV (30), and PTU.RV (33). When comparing the results of PTU treated hearts versus WT for the same ventricle, statistically different results are

indicated by (*) ($0.1 > P \geq 0.05$), *($0.05 > P \geq 0.01$), and **($0.01 > P$). Comparisons were also made between LV and RV for the same treatment group, and statistically different results are indicated by #($0.05 > P \geq 0.01$), and ##($0.01 > P$). The same conventions are used for Figs. 7b, c, 8b, c, and 9c, d

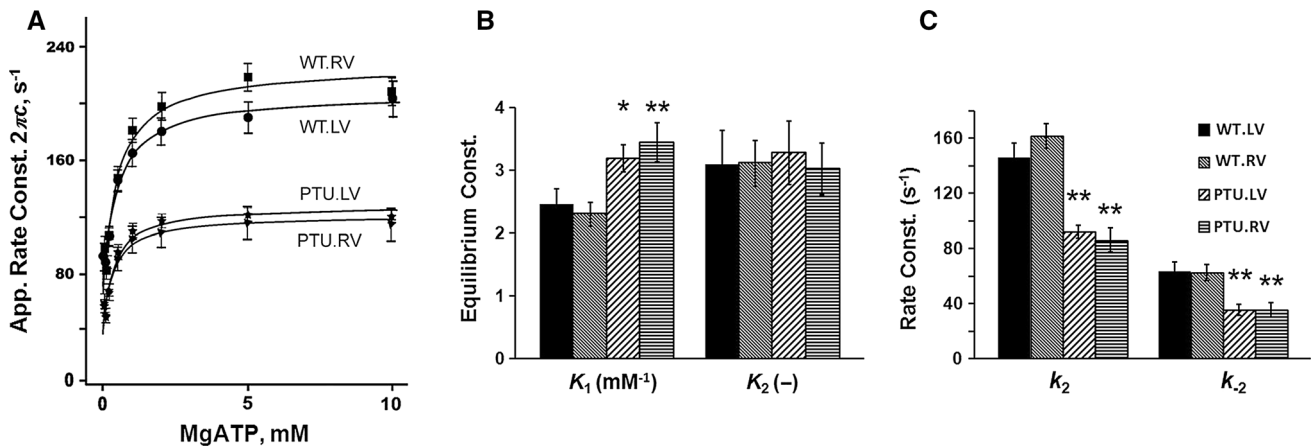


Fig. 7 The ATP study of four kinds of preparations. The number of experiments (*N*) was: WT.LV (17), WT.RV (18), PTU.LV (15), and PTU.RV (18). **a** The apparent rate constant $2\pi c$ is plotted against [MgATP]. Smooth curves represent best fit of the data to Eq. 2: $2\pi c = \frac{K_1 S}{1 + K_1 S} k_2 + k_{-2}$ where $S = [\text{MgATP}]$ (Kawai and Halvorson 1989, 2007). This fitting yields the following kinetic constants: K_1 is the association constant for MgATP to cross-bridge, k_2 is the rate

constant of cross-bridge detachment, and k_{-2} is the rate constant of its reversal step; $K_2 = k_2/k_{-2}$. These are plotted in **b** and **c**. Combined results of LV and RV indicate that K_1 of PTU treated group is significantly different from WT ($P < 0.001$). Similarly, k_2 and k_{-2} of PTU treated group are significantly different from respective values of WT ($P < 0.001$). There was no significant difference between LV and RV

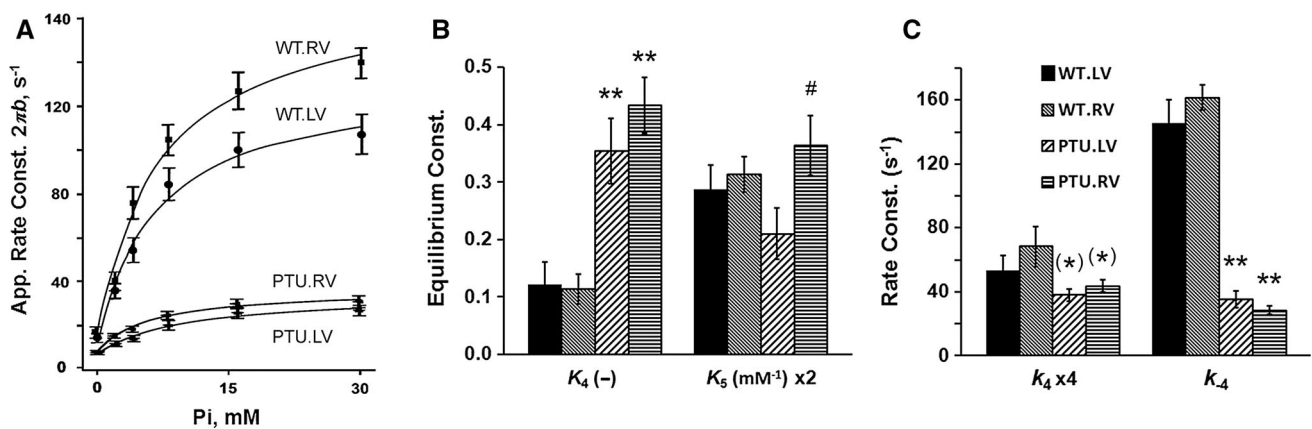


Fig. 8 The Pi study of four kinds of preparations. The number of experiments (*N*) was: WT.LV (17), WT.RV (15), PTU.LV (15), and PTU.RV (19). **a** The apparent rate constant $2\pi b$ is plotted against [Pi]. Smooth curves represent best fit of the data to Eq. 3 (Kawai and Halvorson 1991, 2007), from which the kinetic constants were deduced and plotted in **b** and **c** $2\pi b = \sigma k_4 + \frac{K_5 P}{1 + K_5 P} k_{-4}$ where $\sigma = \frac{K_2 K_1 S}{1 + (1 + K_2) K_1 S}$ σ was calculated based on Eq. 4 with K_1 and K_2

obtained from the ATP study and $S = 5$ mM (experimental condition). k_4 is the rate of force generation step, k_{-4} is its reversal rate, $K_4 = k_4/k_{-4}$, and K_5 is the association constant of Pi to cross-bridge. Combined results of LV and RV indicate that K_4 of PTU treated group is significantly different from WT ($P < 0.001$). Similarly, k_4 and k_{-4} of PTU treated group are significantly different from respective values of WT ($P = 0.016$, $P < 0.001$, respectively). Except for K_5 of PTU treated groups, there was no significant difference between LV and RV

results are plotted in Fig. 7b, c. Figure 7b demonstrates that K_1 of α -MHC is $0.7\times$ of that of β -MHC, but K_2 is not any different between α -MHC and β -MHC. Figure 7c demonstrates that k_2 and k_{-2} from α -MHC are about $2\times$ of those from β -MHC. There are no significant differences between LV and RV in any of the parameters of ATP binding and cross-bridge detachment steps we have examined (Fig. 7b, c).

Pi study

To examine elementary steps surrounding force generation and Pi release from the myosin head, [Pi] was changed in the range 0 mM and 30 mM in the presence of 5 mM MgATP at saturating Ca^{2+} ($p\text{Ca } 4.66$) (Fig. 2b), and the complex modulus data $Y(f)$ were obtained at each [Pi]. The apparent rate constant $2\pi b$ was plotted against [Pi] in Fig. 8a for four

kinds of preparations. As seen in this figure, $2\pi b$ increased at low mM range and then approached saturation at 16–30 mM. $2\pi b$ of α -MHC was significantly larger than that of β -MHC. $2\pi b$ was larger in RV than in LV: their difference was significant in α -MHC, but not significant in β -MHC. These results were fitted to Eq. 3, which is based on steps 4 and 5 of Scheme 1. This fitting characterizes the rate of the force generation step (k_4), its reversal rate (k_{-4}), and the Pi association constant to the myosin head (K_5). Their averaged results are plotted in Fig. 8b, c. As seen in Fig. 8c, k_4 of α -MHC was $1.5\times$ of that of β -MHC, and k_{-4} of α -MHC was $4\text{--}5\times$ of that of β -MHC. This resulted in $0.3\times$ of K_4 in α -MHC compared to β -MHC containing papillary muscle fibers (Fig. 8b). There was no significant difference in K_5 between α -MHC and β -MHC in LV. There were no significant differences between LV and RV for the force generation step 4, but a difference was noticed for Pi-release step 5 of β -MHC: K_5 was significantly larger in PTU.RV than PTU.LV (Fig. 8b). With α -MHC, K_5 was not any different between LV and RV (Fig. 8b).

Ca²⁺ sensitivity and cooperativity

For this study, pCa was changed from 8 to 4.5 (Fig. 2c), active tension was measured, and plotted against pCa in Fig. 9a, b for four kinds of preparations. In these experiments, [MgATP] was 5 mM, [Pi] was 8 mM and the ionic strength was 200 mM, which are the physiological ionic conditions in working cardiomyocytes (Godt and Maughan 1988; Opie et al. 1971; Roth et al. 1989). Tension was at the baseline level for pCa 8–7, started to rise at pCa 6.0, and saturated by pCa 4.5. All four groups expressed pCa_{50} of ~ 5.5 . See Fig. 2c for further experimental details. The pCa -tension plots were individually fitted to Eq. 5. The fitted parameters were averaged, and plotted in Fig. 9c (pCa_{50}) and 9d (n_H). The Ca²⁺ sensitivity appeared to be larger in α -MHC than in β -MHC, and their difference in RV (0.06 pCa unit in RV) was close to a significance ($P = 0.056$), but their difference in LV (0.04 unit) was not significant (Fig. 9c). The cooperativity was in the range 3.0–4.5, it was less in α -MHC than in β -MHC, and their difference was significant ($P = 0.005$) only in RV, but not significant in LV (Fig. 9d). There were no significant differences between the pCa_{50} estimates in fibers from LV and RV from both treatment groups (Fig. 9c). However, PTU treatment abolished any natural differences between the n_H estimates of fibers from normal LV and RV (Fig. 9d).

Discussion

We compared the rat papillary muscle fibers that contained α - and β -MHC, and characterized active tension, stiffness, cross-bridge kinetics, and Ca²⁺ sensitivity. Our results

show that the cross-bridge kinetics are faster in α -MHC than in β -MHC containing fibers as expected from previous studies. By studying the effect of ATP and Pi concentrations, we resolved this difference to the difference in the elementary steps of the cross-bridge cycle. Our results further demonstrate that ATP association constant was larger in β -MHC fibers than in α -MHC fibers. Our results also demonstrate that Ca²⁺ sensitivity, as represented by pCa_{50} , was slightly larger in fibers containing α -MHC than those containing β -MHC. There was not much difference in these parameters comparing LV and RV.

MHC isoforms and difference in LV and RV

With SDS-PAGE analysis, it was shown that LV and RV of WT rat contain $>99\%$ α -MHC ($<1\%$ β -MHC), whereas LV and RV of PTU treated rats contains 100% β -MHC (Fig. 1). Given that the similar MHC composition in LV and RV, we anticipated no major differences in the contractile parameters of fibers from both ventricles. To test this hypothesis, fibers from LV and RV were studied independently. We have compared skinned papillary muscle fibers from WT rat and PTU treated rat in terms of isometric tension, rigor stiffness, cross-bridge kinetics, the parameters of the elementary steps of the cross-bridge cycle, and Ca²⁺ sensitivity. As expected there were no major differences between fibers from LV and RV in any of the parameters studied. A notable exception was the Pi association constant (K_5) of β -MHC containing fibers (Fig. 8b).

Isometric tension and rigor stiffness

There was no difference in active tension (Fig. 3a) or stiffness (Fig. 3b) between fibers containing α - and β -MHC. Also there was no difference in rigor stiffness (Fig. 4). These latter parameters are determined by actomyosin interface and series elasticity of thick and thin filaments. We infer from our findings that there is no change in the actomyosin interface or myosin's series elasticity between fibers containing α -MHC and β -MHC. That is, a difference in actin binding area of myosin (MHC-617-639) in S1, and differences in two LMM segments MHC-1075-1103 and MHC-1249-1276 that form the thick-filament backbone do not contribute to the series elasticity. We do not know the extent of contribution of myosin light chain (MLC) binding segment of myosin (MHC-793-814) to the elasticity at this time. Our observations are in agreement with single molecule studies which demonstrated that neither the unitary force nor the step size is different between α - and β -MHC (Palmiter et al. 1999). Quite expectedly, tension transients were $2\text{--}4\times$ faster in α -MHC containing fibers than β -MHC containing fibers (Fig. 6), and as reported (Michael et al. 2014).

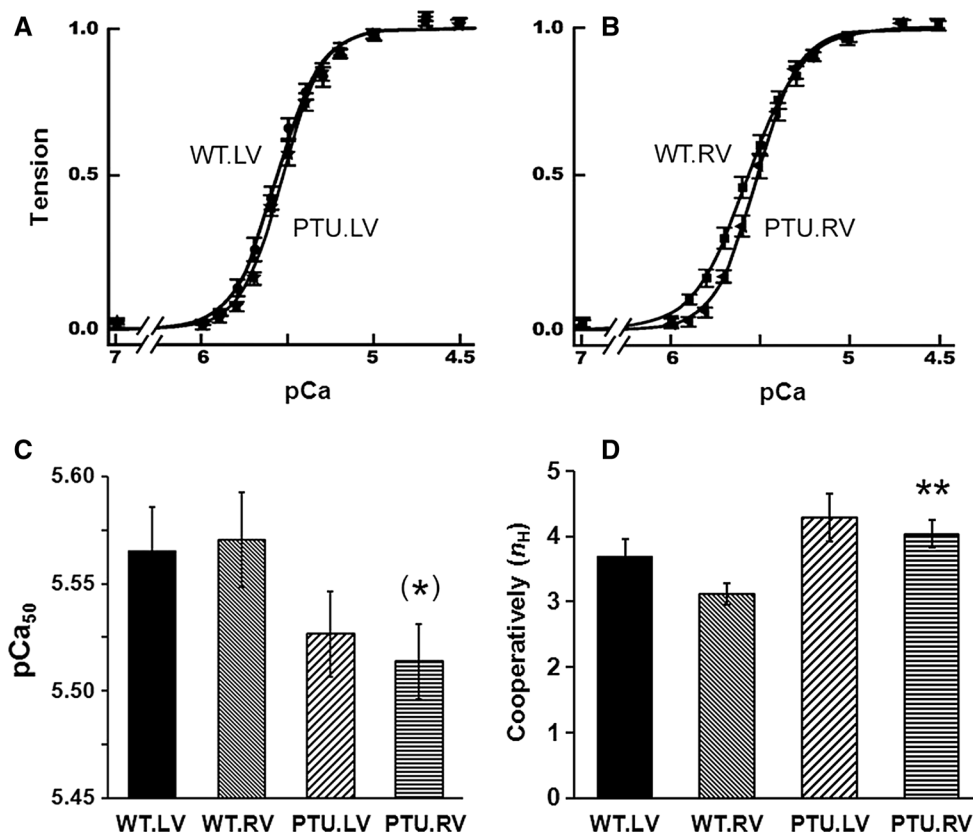


Fig. 9 The results of *pCa*-tension study comparing papillary muscle fibers from WT and PTU-treated rats. Tension was also measured at *pCa* 8, which was not any different from that of *pCa* 7. The number of experiments (*N*) was: WT.LV (13), PTU.LV (14), WT.RV (9), and PTU.RV (18). Papillary fibers from **a** left ventricles (LV), and **b** right ventricles (RV). The data were fitted to Eq. 5 (*smooth curves*) individually. For the actual plotting of the data, *T*₀ found from Eq. 5 was first subtracted from tension data, which were then divided by *T*_m to normalized the data, and then averaged. *Smooth curves* represent best fit of the data to Eq. 5, from which *pCa*₅₀ was deduced and plotted in **c**, and *n*_H in **d**:
$$\text{Tension} = \frac{T_m}{1 + \left(\frac{Ca_{50}}{[Ca^{2+}]}\right)^{n_H}} + T_0$$
 where *Ca*₅₀ is the

apparent Ca²⁺ binding constant, *n*_H is the cooperativity, *T*_m is the maximum (saturating) isometric tension, and *T*₀ is the baseline tension. *pCa*₅₀ (Ca²⁺ sensitivity) is the mid-point of the *pCa*-tension curve, and plotted in **c**. Combined results of LV and RV indicate that *pCa*₅₀ of PTU treated group is significantly different from WT (*P* = 0.021). Similarly, *n*_H (cooperativity) is plotted in **d**. *n*_H of PTU treated group is significantly different from WT (*P* = 0.007). There was no significant difference between LV and RV

Equilibrium constants

The equilibrium constant of ATP association (*K*₁) is significantly (~40%) larger in fibers that contain β-MHC than those that contain α-MHC (Fig. 7b) showing a difference in the affinities of α- and β-MHC cross-bridges to ATP. The binding of ATP to actin-bound cross-bridges causes the cross-bridges to dissociate at the rate constant 2π*c* (Kawai 1978; Kawai and Halvorson 1989). The interpretation of 2π*c* in Wang et al. (2013c) or in Tanner et al. (2014) is slightly different from ours, but by comparing our Eq. 2 and Eq. 3 of Wang et al. (2013c), it can be concluded that *k*₂ corresponds to *k*_{-ADP}, and *K*₁ corresponds to *k*_{+ATP}/*k*_{-ADP}. Thus, from Wang et al. (2013c) *K*₁ = 1.66 mM⁻¹ for α-MHC and 3.54 mM⁻¹ for β-MHC based on their

Table 2, which are not very different from our observations (Fig. 7b). Similar effect of PTU treatment was reported by Tanner et al. (2014). In spite of these differences in the ATP binding step for α-MHC and β-MHC, there is no difference in the amino acid sequence in the nucleotide binding pocket or its nearest neighbor (MHC-160-193) including P-loop (MHC-179-184). However, there is a difference in subsequent segment MHC-196-212 between α-MHC and β-MHC (McNally et al. 1989). Therefore, the difference in the association constant could be caused by this subsequent segment, which may influence the nucleotide binding pocket. The equilibrium constant of the force generation step (*K*₄) were larger in β-MHC than in α-MHC containing fibers (Figs. 7b, 8b). There was no difference in the cross-bridge detachment step (*K*₂). There is a

small effect in the Pi association constant (K_5) in β -MHC (Fig. 8b), if any, which may be the result of the fact that the P-loop is not different at all between α -MHC and β -MHC.

Rate constants

The apparent rate constant $2\pi b$ of fibers containing α -MHC was 4 times faster than that containing β -MHC, and that $2\pi c$ of α -MHC was 2 times faster than that of β -MHC with frequency analysis (Fig. 6). These results correspond well with the faster rate constant of cross-bridge recruitment, detachment (Michael et al. 2016; Stelzer et al. 2007) and ATP hydrolysis rate (Michael and Chandra 2016; Michael et al. 2014); see also Pope et al. (1980). The rate constants (k_2 , k_{-2}) of the cross-bridge detachment step were $1.8\times$ faster in α -MHC fibers than β -MHC fibers (Fig. 7c). It is possible that this difference is caused by the segment MHC-793-814 (McNally et al. 1989), which attaches MLC that may act as a break for the actomyosin interaction Wang et al. (2013a). It is important to note that the role of MLC is to fine-tune the cross-bridge kinetics by its tissue-specific structure (Michael et al. 2012). The current k_2 value in Sprague–Dawley rats compares to the k_{-ADP} value of Wang et al. (2013c), in which they found $4\times$ difference in WKY rats. This difference is presumably caused by the difference in subspecies of the rat. The fact that the current k_2 value is larger than their k_{-ADP} by $2\text{--}4\times$ may be caused by higher temperature (25 vs. 17 °C) as well as the subspecies difference. The rate constant of force generation step (k_4) was $1.3\times$ faster in α -MHC than β -MHC fibers (Fig. 8c). Its reversal step (k_{-4}) was $4\times$ faster in α -MHC than β -MHC fibers (Fig. 8c). This difference may be caused by sequence difference in MHC-617-638 (McNally et al. 1989), which is a part of actin binding segment. Thus, it can be concluded that all four rate constants of the elementary steps of the cross-bridge cycle are faster in fibers containing α -MHC than β -MHC, accounting for the fast kinetics of α -MHC.

Our results on the rate constants are consistent to a recent solution-based study showing that the ATP hydrolysis rate is faster in α -MHC than in β -MHC, affinity to actin is weaker in α -MHC than in β -MHC, the affinity to ADP is weaker in α -MHC than in β -MHC, and the release of ADP is faster in α -MHC than in β -MHC (Deacon et al. 2012); moreover, our results of weaker ATP affinity (Fig. 7b, K_1) are consistent with these observations. Interestingly, the differences between the kinetic constants of α -MHC and β -MHC have been observed across multiple species (Bloemink et al. 2007; Deacon et al. 2012; Millar and Geeves 1988; Ritchie et al. 1993), indicating that the kinetic properties of α -MHC and β -MHC are preserved across species. While structural differences between α - and β -MHC have been attributed to their unique influences in

cross-bridge kinetics, the lack of high-resolution structures of the actin–myosin interface in the physiological conditions preclude greater mechanistic insights.

Ca²⁺ sensitivity

Our results demonstrate that Ca²⁺ sensitivity was slightly larger (by 0.04–0.06 pCa units, or 10–15% in concentration) in fibers containing α -MHC than those containing β -MHC (Fig. 9c). This difference was not significant, and our results are consistent to earlier studies (Fitzsimons et al. 1998; Michael and Chandra 2016; Michael et al. 2014). The small difference may have been caused by an increased phosphorylation of cardiac TnI (Michael et al. 2014) for phosphorylation of cTnI was shown to decrease myofilament Ca²⁺ sensitivity (Layland et al. 2005). The differences in solution compositions may have also contributed to a difference in Ca²⁺ sensitivity; our study used 8 mM Pi in the activating solution, which is physiological (Opie et al. 1971; Roth et al. 1989). Our results also demonstrate that cooperativity is larger in β -MHC containing fibers than in α -MHC containing fibers; this difference was significant in RV, but not as significant in LV (Fig. 9d). These results imply that the regulatory system is affected by the MHC isoform. A possible route for a difference in MHC to affect the regulatory system is through thin filament proteins. This implies that the MHC–actin binding site must be involved. Because MHC-617 through MHC-639 is a part of actin binding site which is different between α -MHC and β -MHC (McNally et al. 1989), we conclude that this segment may be involved for MHC to affect the Ca²⁺ regulatory mechanism. The different influences of α -MHC and β -MHC on cross-bridge kinetics indicate that they may consequently play a differential role in modulating cooperative processes of the thin filament activation.

Conclusions

We have studied the difference in cross-bridge properties including their kinetics between papillary muscle fibers containing α -MHC and β -MHC isoforms. We found no difference in active tension or stiffness, and rigor stiffness, indicating that there is no difference in the actomyosin interface and the series elasticity. In terms of the apparent rate constants ($2\pi b$ and $2\pi c$), fibers containing α -MHC was $2\text{--}4\times$ faster than those containing β -MHC. Similarly, the rate constants (k_2 , k_{-2} , k_4 , k_{-4}) of the elementary steps were $1.3\text{--}4\times$ faster in α -MHC than β -MHC containing fibers. Equilibrium constants of ATP binding (K_1) and the force generation step (K_4) were larger in β -MHC than in α -MHC containing fibers; there was no difference in cross-

bridge detachment step (K_2). A slight reduction in Ca^{2+} sensitivity in fibers containing β -MHC compared to those containing α -MHC was found. Fibers from LV and RV were studied independently, but most parameters were not much different between LV and RV.

Funding This work was supported by a grant from The American Heart Association 13GRNT16810043 to MK, National Heart, Lung, and Blood Institute Grant R01-HL-075643 to MC, and a Poncin Fellowship to JJM.

Compliance with ethical standards

Conflict of interest None.

References

- Andrews MA, Maughan DW, Nosek TM, Godt RE (1991) Ion-specific and general ionic effects on contraction of skinned fast-twitch skeletal muscle from the rabbit. *J Gen Physiol* 98:1105–1125
- Bloemink MJ, Adamek N, Reggiani C, Geeves MA (2007) Kinetic analysis of the slow skeletal myosin MHC-1 isoform from bovine masseter muscle. *J Mol Biol* 373:1184–1197. doi:10.1016/j.jmb.2007.08.050
- Caremani M, Dantzig J, Goldman YE, Lombardi V, Linari M (2008) Effect of inorganic phosphate on the force and number of myosin cross-bridges during the isometric contraction of permeabilized muscle fibers from rabbit psoas. *Biophys J* 95:5798–5808. doi:10.1529/biophysj.108.130435
- Dantzig J, Goldman Y, Millar NC, Lacktis J, Homsher E (1992) Reversal of the cross-bridge force-generating transition by the photogeneration of phosphate in rabbit psoas muscle fibers. *J Physiol* 451:247–278
- Davis JS, Epstein ND (2009) Mechanistic role of movement and strain sensitivity in muscle contraction. *Proc Natl Acad Sci USA* 106:6140–6145. doi:10.1073/pnas.0812487106
- Deacon JC, Bloemink MJ, Rezavandi H, Geeves MA, Leinwand LA (2012) Erratum to: identification of functional differences between recombinant human alpha and beta cardiac myosin motors. *Cell Mol Life Sci* 69:4239–4255. doi:10.1007/s00018-012-1111-5
- Fitzsimons DP, Patel JR, Moss RL (1998) Role of myosin heavy chain composition in kinetics of force development and relaxation in rat myocardium. *J Physiol* 513:171–183. doi:10.1111/j.1469-7793.1998.171by.x
- Ford SJ, Chandra M (2012) The effects of slow skeletal troponin I expression in the murine myocardium are influenced by development-related shifts in myosin heavy chain isoform. *J Physiol* 590:6047–6063. doi:10.1113/jphysiol.2012.240085
- Fortune NS, Geeves MA, Ranatunga KW (1991) Tension responses to rapid pressure release in glycerinated rabbit muscle fibers. *Proc Natl Acad Sci USA* 88:7323–7327
- Galler S, Puchert E, Gohlsch B, Schmid D, Pette D (2002) Kinetic properties of cardiac myosin heavy chain isoforms in rat. *Pflug Arch* 445:218–223. doi:10.1007/s00424-002-0934-6
- Godt RE, Maughan DW (1988) On the composition of the cytosol of relaxed skeletal muscle of the frog. *Am J Physiol* 254:C591–C604
- Heinl P, Kuhn HJ, Ruegg JC (1974) Tension responses to quick length changes of glycerinated skeletal muscle fibres from the frog and tortoise. *J Physiol* 237:243–258
- Huxley AF (1974) Muscular contraction. *J Physiol* 243:1–43
- Kawai M (1978) Head rotation or dissociation?: a study of exponential rate processes in chemically skinned rabbit muscle fibers when MgATP concentration is changed. *Biophys J* 22:97–103
- Kawai M, Brandt PW (1976) Two rigor states in skinned crayfish single muscle fibers. *J Gen Physiol* 68:267–280
- Kawai M, Brandt PW (1980) Sinusoidal analysis: a high resolution method for correlating biochemical reactions with physiological processes in activated skeletal muscles of rabbit, frog and crayfish. *J Muscle Res Cell Motil* 1:279–303
- Kawai M, Halvorson H (1989) Role of MgATP and MgADP in the crossbridge kinetics in chemically skinned rabbit psoas fibers. Study of a fast exponential process C. *Biophys J* 55:595–603
- Kawai M, Halvorson HR (1991) Two step mechanism of phosphate release and the mechanism of force generation in chemically skinned fibers of rabbit psoas. *Biophys J* 59:329–342
- Kawai M, Halvorson HR (2007) Force transients and minimum cross-bridge models in muscular contraction. *J Muscle Res Cell Motil* 28:371–395
- Kawai M, Zhao Y (1993) Cross-bridge scheme and force per cross-bridge state in skinned rabbit psoas muscle fibers. *Biophys J* 65:638–651
- Kawai M, Guth K, Winnikes K, Haist C, Ruegg JC (1987) The effect of inorganic phosphate on the ATP hydrolysis rate and the tension transients in chemically skinned rabbit psoas fibers. *Pflug Arch* 408:1–9
- Kawai M, Saeki Y, Zhao Y (1993) Cross-bridge scheme and the kinetic constants of elementary steps deduced from chemically skinned papillary and trabecular muscles of the ferret. *Circ Res* 73:35–50
- Layland J, Solaro RJ, Shah AM (2005) Regulation of cardiac contractile function by troponin I phosphorylation. *Cardiovasc Res* 66:12–21. doi:10.1016/j.cardiores.2004.12.022
- Lompre AM, Mercadier JJ, Wisnewsky C, Bouveret P, Pantaloni C, D’Albis A, Schwartz K (1981) Species- and age-dependent changes in the relative amounts of cardiac myosin isoenzymes in mammals. *Dev Biol* 84:286–290
- Lu X, Tobacman LS, Kawai M (2006) Temperature-dependence of isometric tension and cross-bridge kinetics of cardiac muscle fibers reconstituted with a tropomyosin internal deletion mutant. *Biophys J* 91:4230–4240. doi:10.1529/biophysj.106.084608
- Malmqvist UP, Aronshtam A, Lowey S (2004) Cardiac myosin isoforms from different species have unique enzymatic and mechanical properties. *Biochemistry* 43:15058–15065. doi:10.1021/bi0495329
- McNally EM, Kraft R, Bravo-Zehnder M, Taylor DA, Leinwand LA (1989) Full-length rat alpha and beta cardiac myosin heavy chain sequences: comparisons suggest a molecular basis for functional differences. *J Mol Biol* 210:665–671
- Michael JJ, Chandra M (2015) Functional effects of the H1-Helix of rat cardiac troponin T on crossbridge detachment rate is differently modulated by α - and β -Myosin heavy chain isoforms. *Biophys J* 108:596a. doi:10.1016/j.bpj.2014.11.3245
- Michael JJ, Chandra M (2016) Interplay between the effects of dilated cardiomyopathy mutation (R206L) and the protein kinase C phosphomimic (T204E) of rat cardiac troponin T are differently modulated by alpha- and beta-myosin heavy chain isoforms. *J Am Heart Assoc* 4:e002777. doi:10.1161/jaha.115.002777
- Michael JJ, Gollapudi SK, Ford SJ, Kazmierczak K, Szczesna-Cordary D, Chandra M (2012) Deletion of 1-43 amino acids in cardiac myosin essential light chain blunts length dependency of Ca^{2+} sensitivity and crossbridge detachment kinetics. *Am J Physiol Heart Circ Physiol* 304:H253–H259. doi:10.1152/ajpheart.00572.2012

- Michael JJ, Gollapudi SK, Chandra M (2014) Effects of pseudo-phosphorylated rat cardiac troponin T are differently modulated by alpha- and beta-myosin heavy chain isoforms. *Basic Res Cardiol* 109:442–457. doi:[10.1007/s00395-014-0442-9](https://doi.org/10.1007/s00395-014-0442-9)
- Michael JJ, Gollapudi SK, Chandra M (2016) Interplay between the effects of a Protein Kinase C phosphomimic (T204E) and a dilated cardiomyopathy mutation (K211Δ or R206 W) in rat cardiac troponin T blunts the magnitude of muscle length-mediated crossbridge recruitment against a β-myosin heavy chain background. *J Muscle Res Cell Motil*. doi:[10.1007/s10974-016-9448-2](https://doi.org/10.1007/s10974-016-9448-2)
- Millar NC, Geeves MA (1988) Protein fluorescence changes associated with ATP and adenosine 5′-[gamma-thio]triphosphate binding to skeletal muscle myosin subfragment 1 and actomyosin subfragment 1. *Biochem J* 249:735–743
- Miller T et al (2001) Abnormal contractile function in transgenic mice expressing a familial hypertrophic cardiomyopathy-linked troponin T (I79 N) mutation. *J Biol Chem* 276:3743–3755. doi:[10.1074/jbc.M006746200](https://doi.org/10.1074/jbc.M006746200)
- Opie LH, Mansford KR, Owen P (1971) Effects of increased heart work on glycolysis and adenine nucleotides in the perfused heart of normal and diabetic rats. *Biochem J* 124:475–490
- Pagani ED, Julian FJ (1984) Rabbit papillary muscle myosin isozymes and the velocity of muscle shortening. *Circ Res* 54:586–594
- Palmiter KA, Tyska MJ, Dupuis DE, Alpert NR, Warshaw DM (1999) Kinetic differences at the single molecule level account for the functional diversity of rabbit cardiac myosin isoforms. *J Physiol* 519(Pt 3):669–678
- Pope B, Hoh JF, Weeds A (1980) The ATPase activities of rat cardiac myosin isoenzymes. *FEBS Lett* 118:205–208
- Ritchie MD, Geeves MA, Woodward SK, Manstein DJ (1993) Kinetic characterization of a cytoplasmic myosin motor domain expressed in *Dictyostelium discoideum*. *Proc Natl Acad Sci USA* 90:8619–8623
- Roth K et al (1989) Noninvasive quantitation of phosphorus metabolites in human tissue by NMR spectroscopy. *J Magn Reson* 81:299–311
- Song W et al (2011) Molecular mechanism of the E99K mutation in cardiac actin (ACTC Gene) that causes apical hypertrophy in man and mouse. *J Biol Chem* 286:27582–27593
- Stelzer JE, Brickson SL, Locher MR, Moss RL (2007) Role of myosin heavy chain composition in the stretch activation response of rat myocardium. *J Physiol* 579:161–173. doi:[10.1113/jphysiol.2006.119719](https://doi.org/10.1113/jphysiol.2006.119719)
- Sweeney HL, Houdusse A (2010) Structural and functional insights into the Myosin motor mechanism. *Annu Rev Biophys* 39:539–557. doi:[10.1146/annurev.biophys.050708.133751](https://doi.org/10.1146/annurev.biophys.050708.133751)
- Tanner BC, Wang Y, Robbins J, Palmer BM (2014) Kinetics of cardiac myosin isoforms in mouse myocardium are affected differently by presence of myosin binding protein-C. *J Muscle Res Cell Motil* 35:267–278. doi:[10.1007/s10974-014-9390-0](https://doi.org/10.1007/s10974-014-9390-0)
- Tesi C, Colomo F, Nencini S, Pirodi N, Poggesi C (2000) The effect of inorganic phosphate on force generation in single myofibrils from rabbit skeletal muscle. *Biophys J* 78:3081–3092
- Wang L, Muthu P, Szczesna-Cordary D, Kawai M (2013a) Characterizations of myosin essential light chain’s N-terminal truncation mutant Delta43 in transgenic mouse papillary muscles by using tension transients in response to sinusoidal length alterations. *J Muscle Res Cell Motil* 34:93–105. doi:[10.1007/s10974-013-9337-x](https://doi.org/10.1007/s10974-013-9337-x)
- Wang L, Muthu P, Szczesna-Cordary D, Kawai M (2013b) Diversity and similarity of motor function and cross-bridge kinetics in papillary muscles of transgenic mice carrying myosin regulatory light chain mutations D166V and R58Q. *J Mol Cell Cardiol* 62:153–163
- Wang Y et al (2013c) Cardiac myosin isoforms exhibit differential rates of MgADP release and MgATP binding detected by myocardial viscoelasticity. *J Mol Cell Cardiol* 54:1–8. doi:[10.1016/j.yjmcc.2012.10.010](https://doi.org/10.1016/j.yjmcc.2012.10.010)
- Wang L, Sadayappan S, Kawai M (2014) Cardiac myosin binding protein C phosphorylation affects cross-bridge cycle’s elementary steps in a site-specific manner. *PLoS ONE* 0113417:1–21
- Wannenburg T, Heijne GH, Geerdink JH, Van-Den-Dool HW, Janssen PM, DeTombe PP (2000) Cross-bridge kinetics in rat myocardium: effect of sarcomere length and calcium activation. *Am J Physiol* 279:H779–H790
- Wolska BM et al (1999) Correlation between myofilament response to Ca²⁺ and altered dynamics of contraction and relaxation in transgenic cardiac cells that express beta-tropomyosin. *Circ Res* 84:745–751